

## Sb RECOVERY FROM AN As PRE-REMOVED LEAD ANODE SLIME USING A ZnS-Na<sub>2</sub>CO<sub>3</sub> SMELTING REDUCTION

Z.-Q. Dong <sup>a,b</sup>, R. Zhang <sup>c</sup>, Y.-X. Sun <sup>c</sup>, Z.-D. Gu <sup>c</sup>, X.-Y. Guo <sup>a,\*</sup>, Lei Li <sup>c,\*\*</sup>, S.-S. Wang <sup>a</sup>

<sup>a</sup> Central South University, School of Metallurgy and Environment, Changsha, China

<sup>b</sup> Shandong Humon Smelting CO., LTD, Yantai, China

<sup>c</sup> Donghua University, College of Environmental Science and Engineering, Shanghai, China

(Received 30 December 2023; Accepted 27 June 2024)

### Abstract

Lead anode slime is produced in large quantities during lead electrolysis, which has a high Sb content of 10-50 wt% and can be easily recycled. However, in a general alkaline pressure leaching process for pre-removal of As, Sb was partially converted to Na<sub>3</sub>SbO<sub>4</sub> with high stability. This limited the Sb reduction and recovery in the subsequent Na<sub>2</sub>CO<sub>3</sub> smelting reduction. Considering this fact, ZnS was creatively used as an additive in this study to destroy the stable structure of Na<sub>3</sub>SbO<sub>4</sub> and increase Sb reduction, and meanwhile ZnS was reduced to volatile Zn (g) and recycled. In a certain range, increasing the amount of coke and ZnS increased the Sb yield, and Pb recycling could be accelerated. However, when an excessive amount of ZnS was added, the Sb compounds could be sulfurized and then combined with the generated PbS and Na<sub>2</sub>S, forming a sodium matte of Na-Pb-Sb-S. This limited the Sb reduction and reduced the Sb yield. Under the optimum conditions of a coke content of 13%, a ZnS/Sb molar ratio of 0.32, a smelting temperature of 1200 °C and a holding time of 90 min, Sb, Pb and Zn yields of up to 94.8%, 96.1% and 98.9%, respectively, were obtained.

**Keywords:** As pre-removed lead anode slime; Sb recovery; ZnS; Phase transformation; Smelting reduction

### 1. Introduction

Antimony (Sb) is a rare silvery white metal, possessing the characteristics of thermal expansion, cold contraction and strong corrosion resistance [1]. It is an irreplaceable material for the modern industrial, which could be used in the production of flame retardant, alloys, glass and semiconductor components etc. [2]. However, the Sb abundance in the earth crust was low to 0.2-0.5 ppm, and it has been deeply mined world-widely [3]. The Sb supply is expected to approach a critical level in the future, causing the recycling of Sb-bearing secondary resources to be a strong driving force of economic growth and environment safety.

There is a wide variety of Sb-bearing secondary resources, including arsenic-alkali residue, arsenic-antimony dust, waste alloys, and lead anode slimes, etc. [4-6]. Among them, the lead anode slime, which is produced in a lead electrolysis process, has become the focus of research recently [7], ascribed to its huge amounts, high contents of Sb (10 wt%-50 wt%), Pb (5 wt%-25 wt%) and noble metals (Au, Ag etc.). The output of lead anode slimes occupies the proportion of 1.3% - 2% of the refined Pb (Peng, 2012). Moreover,

the high proportion of harmful element of As that is contained in lead anode slimes leads to its high toxicity. It is of great significance to separate and extract Sb from lead anode slimes, which could relieve the Sb mineral resource pressure. Sb existed mainly in the forms of Sb, Sb<sub>2</sub>O<sub>3</sub>, SbAsO<sub>4</sub> and Ag<sub>2</sub>Sb in the lead anode slime [8]. Based on this, the Sb extraction methods from lead anode slimes could be divided into pyro-metallurgical, hydro-metallurgical and combined processes at present [9]. In the pyro-metallurgical process, the lead anode slime was treated using a direct smelting reduction, in which the Sb oxides were reduced and combined with the reduced Pb to form a Pb-Sb alloy, rendering it recovery [10]. Although a high Sb yield can be acquired, massive As from lead anode slimes were reduced simultaneously and entered into the Pb-Sb alloy, causing a difficulty for the Sb further separation [11]. Hydro-metallurgical process generally employed hydrochloric acid and ferric chloride as leaching agents to transfer Sb oxides to a soluble SbCl<sub>3</sub>, and then a chemical precipitation was used to concentrate the generated SbCl<sub>3</sub> into a Sb-containing sediment [12-14]. After a pressure filtration processing, Sb could be recovered. The Sb recovery rate obtained up to 99.98% in the hydro-metallurgical

Corresponding author: xyguo@csu.edu.cn \*; tianxiametal1008@dhu.edu.cn \*\*;

<https://doi.org/10.2298/JMMB231230017D>



process, while the elements of Pb, As and Bi were leached simultaneously and a further precipitation was required. This obviously increased the consumption of chemical agents and the processing cost. In the combined process of hydro- and pyro-metallurgy, an alkaline pressure leaching was firstly performed to selective leach As from Sb, Pb and Bi, realizing their effective separation and recovery [15]. Specifically, As and Sb could be oxidized to high valence states in the pressure leaching. In the presence of alkaline, the As oxides of high valence state dissolved into the leach liquor, while the Sb oxides did not dissolve and entered the leaching residue in the forms of  $\text{Bi}_3\text{SbO}_7$ ,  $\text{Na}_3\text{SbO}_4$  and  $\text{Sb}_2\text{O}_5$  etc [16]. Then in the smelting reduction of the leaching residue,  $\text{Na}_2\text{CO}_3$  was used as slagging agent and the Sb oxides were reduced and recovered in the form of Pb-Sb alloy [17]. It might be more appropriate to realize the efficient recovery of Sb from lead anode slimes, considering that the As could be pre-removed. However, in the smelting reduction, the obtained  $\text{Na}_3\text{SbO}_4$  from the alkaline pressure leaching was hard to be deeply reduced, due to the low reductive activity of sodium salts [18]. It caused that the Sb content in the smelting slag achieved up to 3.8 wt%-4.5 wt% [19] and the Sb yield was low around 80%. How to perform the deep reduction of the alkaline leaching residue has come to a focal issue.

Based on previous research, sulfides could destruct the stable structure of sodium salts via transforming the 'Na' component in it to  $\text{Na}_2\text{S}$  [20], which in turn increased the reductive activity of sodium salts. Considering this, ZnS was used as an additive to promote the reduction of  $\text{Na}_3\text{SbO}_4$  and increase the Sb yield from the As pre-removed lead anode slime (ARLAS) in this research. Besides, the Pb recovery and Zn recycling from the added ZnS were also focused. The influences of parameters of ZnS amount, smelting temperature and holding time were systematically studied. The phase transformations of Pb and Sb during the performance of this process were investigated using X-ray diffraction (XRD) and scanning electron microscopy coupled with energy-dispersive X-ray spectroscopy (SEM-EDS).

## 2. Experimental

### 2.1. Materials

The As pre-removed lead anode slime (ARLAS) used in this study was provided by a lead smelter locating in Shandong province of China. The contents

of Sb, Pb, Bi, Au and Ag in it were 29.88 wt%, 13.14 wt%, 4.52 wt%, 528 g/t and 68800 g/t respectively (Table 1), indicating its high value and possibility to be recycled. Bi, Au and Ag have been efficiently recovered from the ARLAS in previous research [21], and their behavior was not focused in this study. The XRD pattern of the ARLAS was given in Figure 1, which showed that the Pb- and Sb-containing phases were  $\text{Pb}_2\text{Sb}_2\text{O}_7$ ,  $\text{Bi}_3\text{SbO}_7$ ,  $\text{Na}_3\text{SbO}_4$  and  $\text{Sb}_2\text{O}_3$  respectively. Table 2 presented the Sb phase distribution, in which  $\text{Na}_3\text{SbO}_4$  occupied 25.1% of the total Sb phases. The XPS result of Sb 3d from the ARLAS in Figure 1(b) presented that the Sb phases were composed of Sb (III) and Sb (V) compounds, which was consistent with the XRD result in Figure 1(a).

Besides, coke was used as reductant and its composition is listed in Table 3. The chemical reagents used, including ZnS and  $\text{Na}_2\text{CO}_3$ , were of analytical grade and purchased from Shanghai Chemical Reagent Company. The purity of Ar used in this study were higher than 99.99 vol%.

**Table 1.** Chemical composition of the As pre-removed lead anode slime (wt%)

Element	Na	Pb	Sb	Bi	As	Ag	Au
Content	4.32	13.14	29.88	4.52	6.53	68.8kg/t	528g/t

\*Pb, Sb, As and Bi contents were determined using chemical analysis methods, and Na, Au and Ag contents were detected via inductively coupled plasma optical emission spectrometry (ICP-OES, Analytik Jena AG)

**Table 2.** Sb compositions in the As pre-removed lead anode slime acquired via XRD calculation of Figure 1(a) (wt%)

Distribution (%)					
$\text{Sb}_2\text{O}_3$	$\text{Na}_3\text{SbO}_4$	$\text{Pb}_2\text{Sb}_2\text{O}_7$	$\text{Bi}_3\text{SbO}_7$	Others	Total
50.2	25.1	13.7	6.8	4.2	100

### 2.2. Experimental Methods

A vertical electric resistance tube furnace (OTF-1600X, Hefei Kejing Materials Technology Co. Ltd., China) was employed for the tests in this study, as presented in Figure 2. The temperature was measured via a Pt-Rh thermocouple and controlled by a KSY Intelligent Temperature Controller. To increase the contact among the ARLAS, coke, ZnS and  $\text{Na}_2\text{CO}_3$ ,

**Table 3.** Industrial analysis of coke and chemical composition of the ash (wt%)

Industrial analysis				Chemical composition of the ash in the coke					
$\text{FC}_{\text{ad}}$	$\text{M}_{\text{ad}}$	$\text{A}_{\text{ad}}$	$\text{V}_{\text{ad}}$	S	P	$\text{SiO}_2$	$\text{Al}_2\text{O}_3$	MgO	CaO
81.7	4.2	11.8	2.3	0.80	0.02	6.17	1.34	0.65	1.57



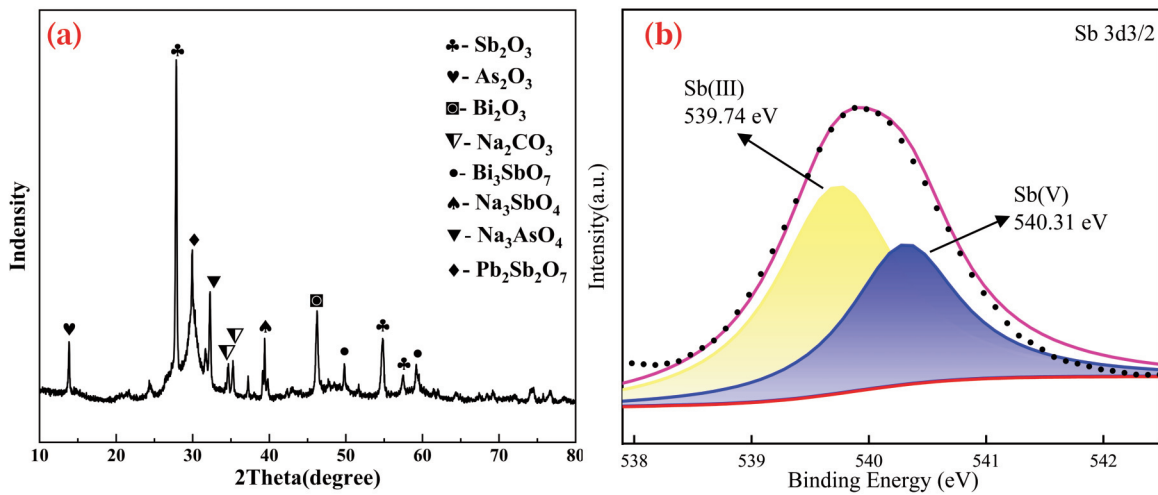


Figure 1. (a) XRD pattern of the As pre-removed lead anode slime; (b) XPS spectra of the As pre-removed lead anode slime at Sb 3d3/2

their particle sizes were all controlled to be lower than 75  $\mu\text{m}$ . The amount of coke or  $\text{Na}_2\text{CO}_3$  added was expressed as the mass ratio of coke/ $\text{Na}_2\text{CO}_3$  to the ARLAS respectively. The amount of ZnS used was defined as the ZnS/Sb molar ratio. The  $\text{Na}_2\text{CO}_3$  amount was chosen as 20% in this study, aiming to decrease the slag viscosity and increase the separation of metal from molten slag [22]. After that the ARLAS, coke, ZnS and  $\text{Na}_2\text{CO}_3$  were thoroughly mixed, they were placed in a corundum crucible and later in the vertical resistance for heating to a proper temperature in pure  $\text{N}_2$  atmosphere at a flow rate of 40 mL/min. In pure  $\text{N}_2$  atmosphere, the target temperature was held for a certain time, and then the sample was cooled

down to room temperature. At last, the obtained metal ingot and slag were separated and prepared for analysis. Besides, the exhaust gases released during the tests were absorbed by a NaOH solution.

### 2.3. Characterization

The elemental composition of the sample was determined using an inductively coupled plasma optical emission spectrometer (ICP-OES, Analytik Jena AG) and chemical analysis. These measurements were performed three times, and the average value was taken as the final result. X-ray diffraction (XRD, Rigaku, TTR -III) was used to detect the sample phase

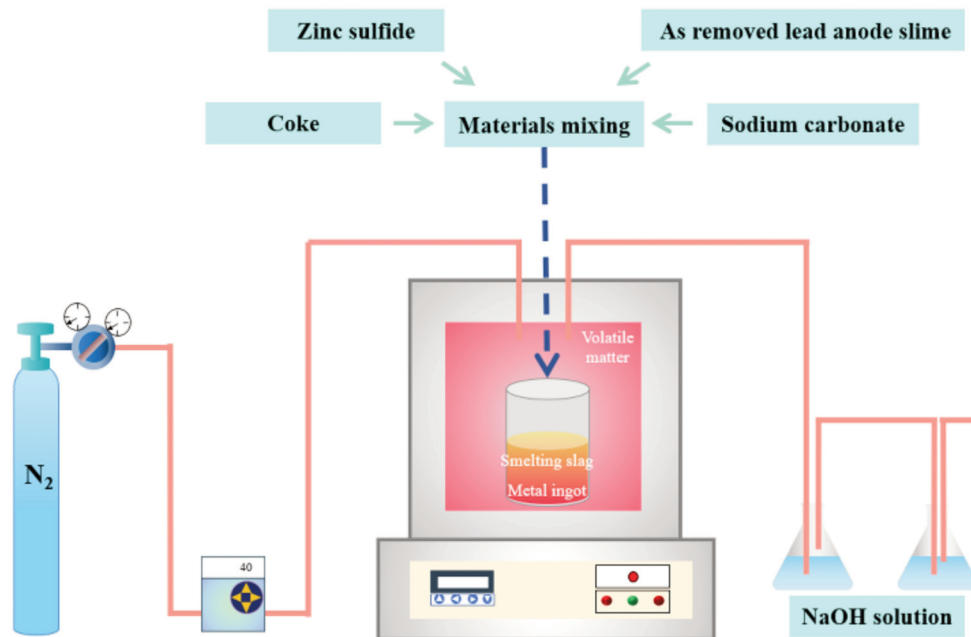


Figure 2. The schematic diagram of experimental apparatus

composition, and its pattern was obtained using Cu-K $\alpha$  radiation in the  $2\theta$  range of  $10^\circ$ – $80^\circ$  with a scan step of  $2^\circ/\text{min}$ . SEM-EDS analysis was used to characterize the microstructure and phase distribution of the sample. In the SEM-EDS analysis, the sample was gold-coated, embedded in resin, and polished for precise measurement.

In this study, the Zn yield from the added ZnS was calculated using Eq. (I).

$$R_{Zn} = 1 - m_2 c_{Zn}'' / m_{ZnS} c_{Zn} - m_1 c_{Zn}' / m_{ZnS} c_{Zn} \quad (I)$$

Where  $m_{ZnS}$ ,  $m_1$  and  $m_2$  represent the mass of the added ZnS, the obtained smelting slag and metal ingot, respectively;  $c_{Zn}$ ,  $c_{Zn}'$  and  $c_{Zn}''$  represent the Zn content in the added ZnS, smelting slag and metal ingot, respectively.

The recovery percentages of Sb ( $R_{Sb}$ ) and Pb ( $R_{Pb}$ ) from the ARLAS were both calculated using Eq. (II).

$$R_{Sb/Pb} = m_2 c_2 / m_0 c_0 \quad (II)$$

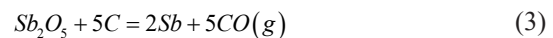
where  $m_0$  represent the mass of the original ARLAS;  $c_0$  and  $c_2$  represent the Sb and Pb contents in the original ARLAS and metal ingot, respectively.

### 3. Thermodynamic analysis

Bi, Au and Ag have been efficiently recovered from the ARLAS using a pyrometallurgy process as reported in previous research [23], and their behavior was not focused in this study. As presented in Figure 1, Sb existed in the forms of  $Pb_2Sb_2O_7$ ,  $Bi_3SbO_7$ ,  $Na_3SbO_4$  and  $Sb_2O_3$  in the ARLAS.  $Pb_2Sb_2O_7$  and  $Bi_3SbO_7$  would be firstly decomposed to  $Sb_2O_5$ , PbO and  $Bi_2O_3$  by Eqs. (1)-(2) in a smelting reduction [24]. Then  $Sb_2O_5$ ,  $Na_3SbO_4$  and  $Sb_2O_3$  were reduced via Eqs. (3)-(5) in a general  $Na_2CO_3$  smelting reduction [25]. Figure 3(a) presented that Eqs. (3)-(5) could be carried out thermodynamically, due to their negative stand Gibbs free energies. However, in the actual production, the Sb content in the smelting slag achieved up to 3.8 wt%-4.5 wt% [26]. The reason might be that the reduction of  $Na_3SbO_4$  could be divided into two stages of the generation of Sb via Eq. (6) and then the formation of  $Na_2CO_3$  by Eq. (7).

It is noteworthy that the standard Gibbs free energy ( $\Delta G^\theta$ ) of Eq. (6) was positive (Fig. 3(a)), indicating that it was hardly to be deeply performed. The  $CO_2$  consumption using Eq. (7) could promote the occurrence of Eq. (6) based on the results in Figures 3(a) and (b). Figure 3(a) showed that Eq. (7) could be carried out thermodynamically, which could decrease the  $CO_2$  partial pressure and in turn promote the performance of Eq. (6) seen from Figure 3(b). While, the  $CO_2$  consumption and the formation of  $Na_2CO_3$  was limited at a low  $CO_2$  partial pressure

(Fig. 3(b)), which would restrict the  $Na_3SbO_4$  reduction from the viewpoint of chemical equilibrium and cause a Sb loss in the slag. To increase the reduction of  $Na_3SbO_4$  and the Sb yield, ZnS was used as an additive to convert the ‘Na’ in  $Na_3SbO_4$  to  $Na_2S$  and in sequence increase the Sb reductive activity in this research. Figure 3(a) showed that as the temperature exceeded  $900^\circ C$ , the stand Gibbs free energy of the  $Na_3SbO_4$  reduction in the presence of ZnS (Eq. (8)) had an obvious decrease compared to that of the direct carbothermal reduction (Eq. (4)). It indicated the acceleration effect of ZnS. In addition, the generated CO (g) evaporated into the gas in the smelting reduction, which further decreased the Gibbs free energy of Eq. (8) and promoted it to occur as presented by Figure 3(c). It is noteworthy that the added ZnS was reduced to a gaseous Zn (g) in Eq. (8) and then could be recycled through a dust collection. In other words, the Zn from the ZnS would not be lost in this proposed process. Figure 3(d) presented the phase equilibrium composition of Eq. (8) at different temperatures. It could be seen that the increase of temperature accelerated the  $Na_3SbO_4$  reduction, and a complete reduction could not be achieved until the temperature reached  $1500^\circ C$ . While, in the presence of more the C amount, the reduction potential of the reaction system could be increased and the temperature required for the  $Na_3SbO_4$  complete reduction could be decreased to  $1000^\circ C$  (Fig. 3(e)). An excessive coke should be added in this ZnS- $Na_2CO_3$  smelting reduction. Besides, the PbO generated from Eq. (1) could be reduced into Pb simultaneously via Eq. (9) and then combined with the reduced Sb to form a Pb-Sb alloy by Eq. (10), which also benefited the  $Na_3SbO_4$  reduction according to the Raoult’s law [16]. In the Raoult’s law, the activity of Sb in the Pb-Sb alloy melt decreased with the decrease of Sb content in the Pb-Sb alloy melt. As more the PbO was reduced and entered into the Pb-Sb alloy, the Sb content in the Pb-Sb alloy melt decreased, resulting in the decrease of Sb activity in the alloy melt. It accelerated the  $Na_3SbO_4$  reduction from the perspective of chemical equilibrium. After  $Na_2S$  was formed via Eq. (8), it entered into the slag and in sequence a  $Na_2S$ - $Na_2CO_3$  slag was formed. Figure 3(f) showed the binary phase diagram of  $Na_2S$ - $Na_2CO_3$ , in which the  $Na_2S$ - $Na_2CO_3$  melt located in liquid state as the temperature exceeded  $1180^\circ C$ . Temperature played an important role on the  $Na_3SbO_4$  reduction and then Sb separation from molten slag in the proposed ZnS- $Na_2CO_3$  smelting reduction.



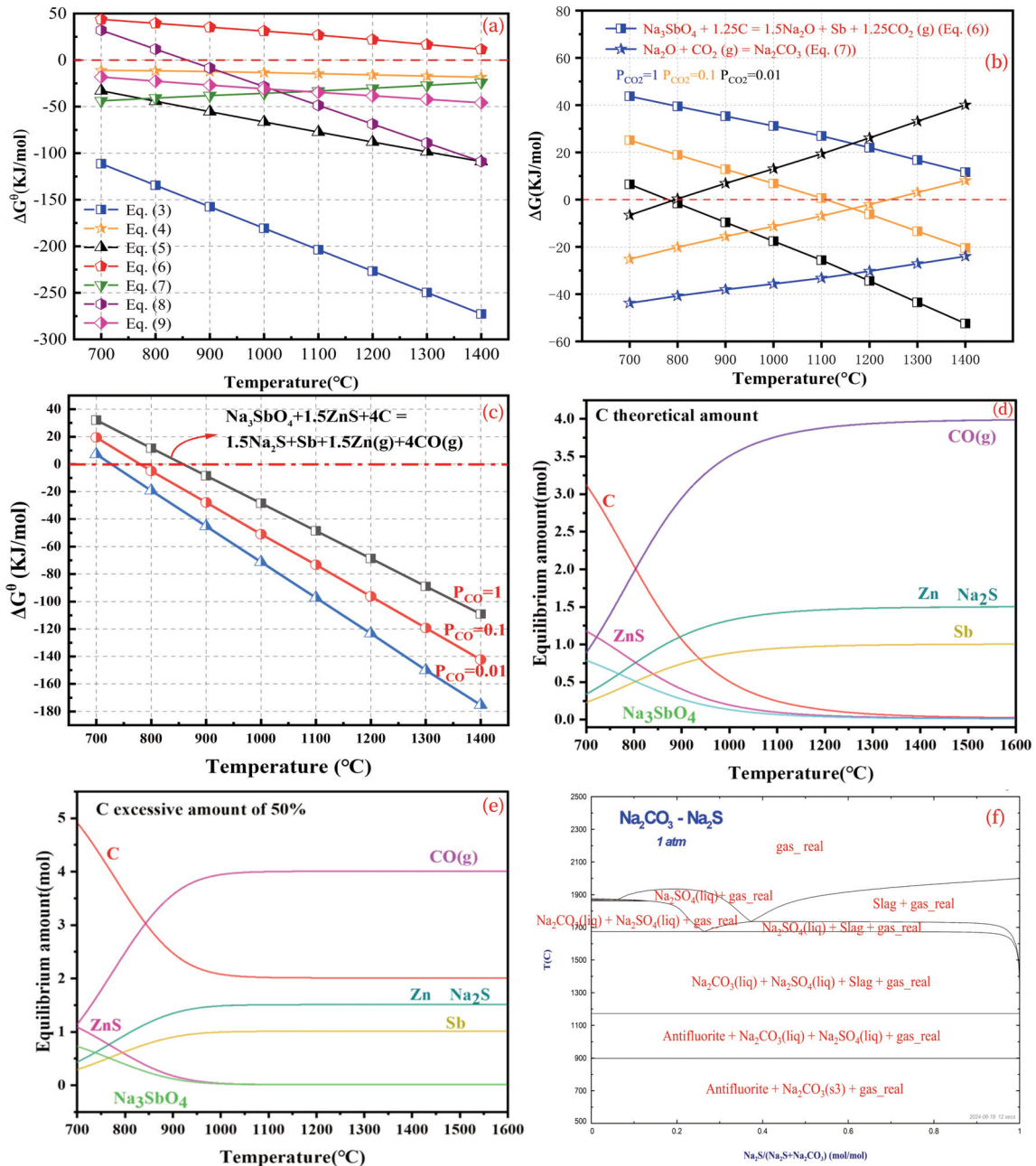
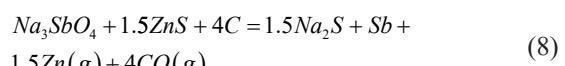
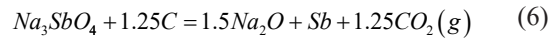
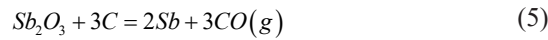
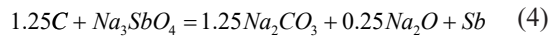


Figure 3. (a) Changes of standard Gibbs free energy ( $\Delta G^0$ ) of Eqs. (3)-(9) with temperature; (b) Changes of Gibbs free energy ( $\Delta G$ ) of Eq. (6) and Eq. (7) at different  $CO_2$  partial pressures ( $P_{CO_2}$ ) with temperature (c) Changes of Gibbs free energy ( $\Delta G$ ) of Eq. (8) at different  $CO$  partial pressures ( $P_{CO}$ ) with temperature; (d) Equilibrium compositions of Eq. (8) with the theoretical C amount at different smelting temperatures; (e) Equilibrium compositions of Eq. (8) with the C excessive amount of 50% at different smelting temperatures; (f) Binary phase diagram of  $Na_2S$ - $Na_2CO_3$  at different temperatures



## 4. Results and discussion

### 4.1. Effects of coke addition amount

Under the conditions of the ZnS/Sb molar ratio of 0.32,  $\text{Na}_2\text{CO}_3$  amount of 20 %, smelting temperature of 1200 °C and holding time of 120 min, the effects of coke amount on the Sb yield from the ARLAS were firstly studied. Besides, the recycling of Pb and Zn were also focused.

In Figures 4(a) and (b), when the coke amount increased from 5.0% to 13.0%, the Sb and Pb yields increased and their respective contents in the smelting slag decreased. The reason was that as more the reductant of coke added, more the  $\text{Pb}_2\text{Sb}_2\text{O}_7$ ,  $\text{Bi}_3\text{SbO}_7$ ,  $\text{Na}_3\text{SbO}_4$  and  $\text{Sb}_2\text{O}_3$  in the ARLAS could be reduced and recovered in the form of Pb-Sb alloy using Eqs. (1)-(3), (5) and (8)-(10). However, when the coke amount increased further to 14%, a phase of C could be detected in the smelting slag (Fig. 5(a)), which has been shown to cause a high viscosity and poor fluidity of the molten slag based on previous research [26]. It hindered the separation of the obtained Pb-Sb alloy from molten slag and decreased the Pb and Sb yields, as presented in Figure 4(a). Besides, C also entered into the obtained Pb-Sb alloy as indicated by the composition of point 'A' in Figure 5(b). It could increase the alloy melting point [27], further decreased its separation from slag and increased the Pb and Sb contents in the smelting slag (Fig. 4(b)). It is noteworthy that a phase of  $\text{Na}_2\text{S}$  was detected in the smelting slag (Fig. 5(a)) and the Sb oxides have been reduced to metallic Sb (Fig. 5(b)). This phase evolution confirmed the occurrence of Eq. (8). The coke amount of 13.0% was proved optimal for enhancing the recycling of Sb and Pb. Besides, it is noteworthy that the Zn content in the smelting slag was low to 0.31 wt% at this coke amount (Fig. 4(b)),

indicating that the added ZnS was efficiently reduced to Zn (g) using Eq. (8) and then volatilized. The volatilized Zn (g) could be recycled using a dust collection.

### 4.2. Effects of ZnS addition amount

At the conditions of coke amount of 13%,  $\text{Na}_2\text{CO}_3$  amount of 20 %, smelting temperature of 1200 °C and holding time of 120 min, the effects of ZnS amount on the Sb yield from the ARLAS were studied.

In the absence of ZnS, the deep reduction of  $\text{Na}_3\text{SbO}_4$  was limited based on the thermodynamic analysis in Figures 3(a), and it could be confirmed by the SEM-EDS result of the smelting slag in Figure 6(a). Figure 6(a) presented that some  $\text{Na}_3\text{SbO}_4$  were not reduced and remained in the slag, which caused that the Sb residual content reached 3.63 wt% in Figure 7(a). When ZnS was added and its amount increased, the reduction of  $\text{Na}_3\text{SbO}_4$  could be accelerated via Eq. (8) as indicated by Figures 3 (a) and (c). Concretely, the transformation of  $\text{Na}_3\text{SbO}_4$  to  $\text{Sb}_2\text{O}_5$  by Eq. (11) and then the  $\text{Sb}_2\text{O}_5$  reduction to metallic Sb via Eq. (3) were promoted. As a result, the Sb recovery rate increased from 80.3% to 94.8 % and its content in the smelting slag decreased from 3.63 wt% to 1.21 wt% as the ZnS/Sb molar ratio changed from 0.00 to 0.32 in Figures 7(a) and (b). In addition, the Pb yield and the Pb content in the smelting slag also presented a similar variation trend in this range of ZnS/Sb molar ratio (Figs. 7(a)&(b)). As described in Eq. (10), after that the metallic Pb and Sb were obtained from the smelting reduction, they would be combined into a Pb-Sb alloy. More the reduction of  $\text{Na}_3\text{SbO}_4$  would cause more the produced Sb to enter into this Pb-Sb alloy, and the Pb content in the Pb-Sb alloy decreased with it. It decreased the Pb activity in

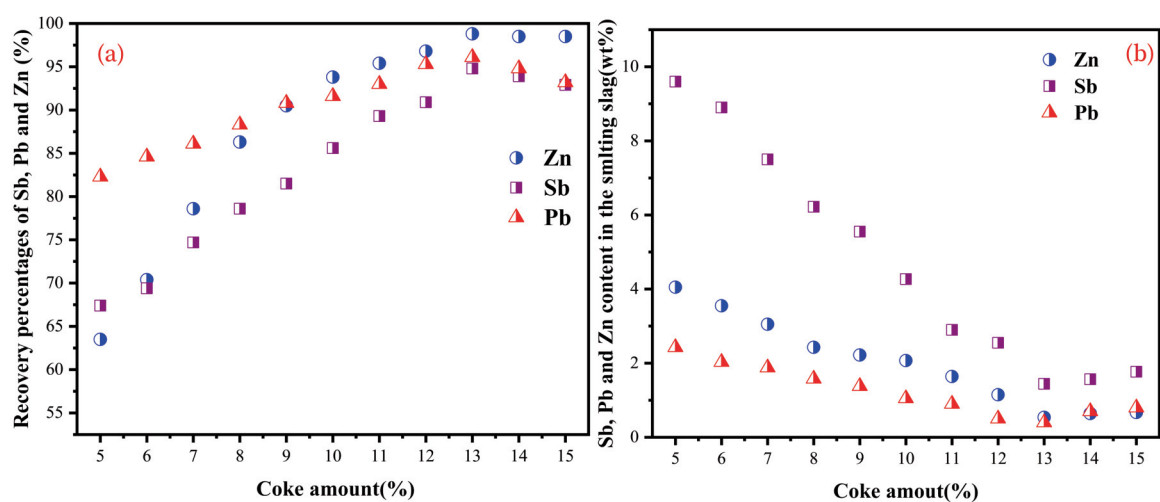


Figure 4. (a) Effects of coke amount on the Sb, Pb and Zn recovery percentages from the As pre-removed lead anode slime; (b) Effects of coke amount on the Sb, Pb and Zn contents in the smelting slag



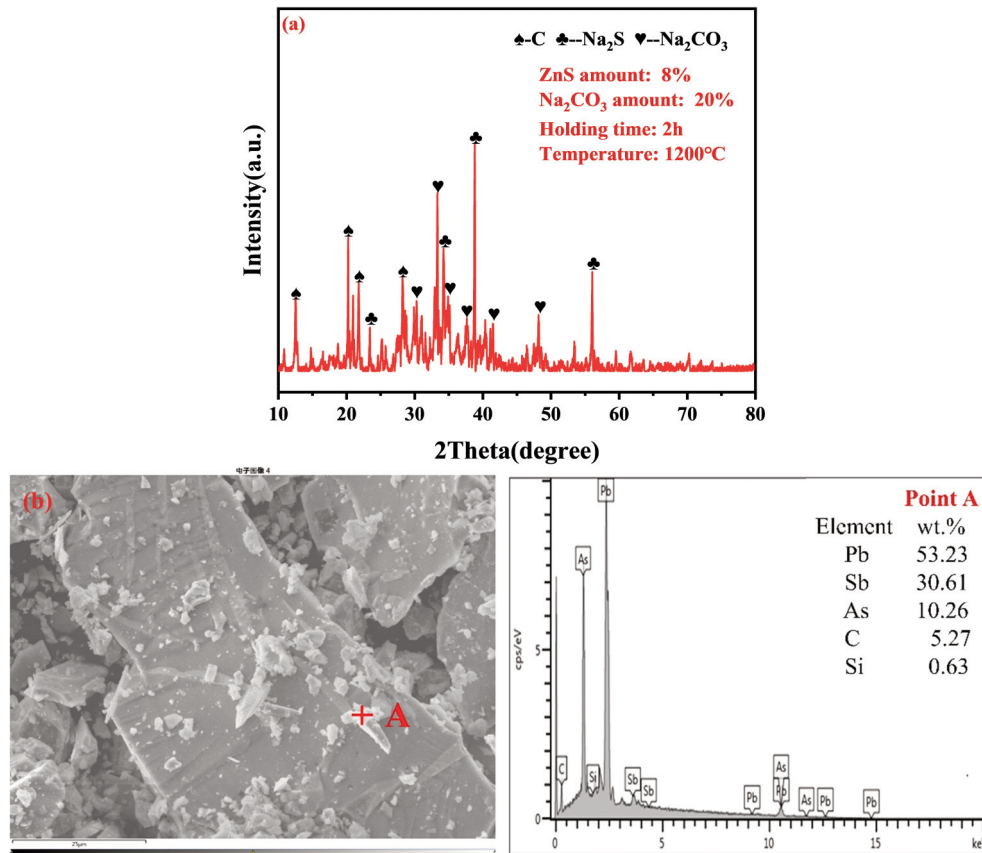
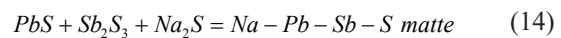
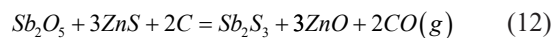
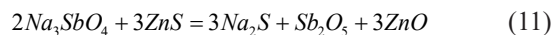


Figure 5. (a) XRD pattern of the smelting slag obtained at the coke amount of 14%; (b) SEM-EDS result of the smelting slag obtained at the coke amount of 14%

the Pb-Sb alloy according to the Raoult's law, which in turn accelerated the Pb reduction (Fig. 7(c)) and increased the Pb yield.

However, as the ZnS amount increased further, the generated  $Sb_2O_5$  from Eq. (11) could be sulfurized to  $Sb_2S_3$  by ZnS using Eq. (12), and then combined with the generated PbS via Eq. (13) and  $Na_2S$  to form a sodium matte known as Na-Pb-Sb-S using Eq. (14). The element composition of the point "2" in Figure 6(b) confirmed the generation of this sodium matte. Besides, Figure 7(d) indicated the feasibility of Eqs. (12) and (13) attributed to their stand negative Gibbs free energies. The generated sodium matte limited the reduction of PbS and  $Sb_2S_3$  based on previous research [28], and as a result the Pb and Sb yields decreased and their contents in the smelting slag increased in Figures 7(a) and (b) respectively. Besides, the reduction of ZnS was also hindered, and its recycling was decreased (Figs. 7(a)&(b)). The ZnS/Sb molar ratio amount was optimized to be 0.32 to increase the recycling of Pb, Sb and Zn.



#### 4.3. Effects of smelting temperature and time

Under the conditions of coke amount of 13%,  $Na_2CO_3$  amount of 20 % and ZnS/Sb molar ratio of 0.32, the effects of smelting temperature and holding time on the Sb yield from the ARLAS were studied.

As depicted in Figure 3(f), the temperature affected the  $Na_2S$ - $Na_2CO_3$  slag phase composition. It further affected the physicochemical property of the molten slag according to previous research, including its viscosity, surface tension and oxidation-reduction potential etc. [29]. This would finally influence the Pb, Sb and Zn yields from the slag. Specifically, the increase in temperature promoted the reduction of  $Sb_2O_3$ ,  $Pb_2Sb_2O_7$ ,  $Bi_3SbO_7$  and  $Na_3SbO_4$  from the ARLAS according to Figure 3(a) and then increased the separation of the obtained Pb-Sb alloy from molten slag by decreasing the slag viscosity. As a result, the Pb and Sb recovery percentages increased from 80.4 % to 96.1 % and from 66.5 % to 94.8 %

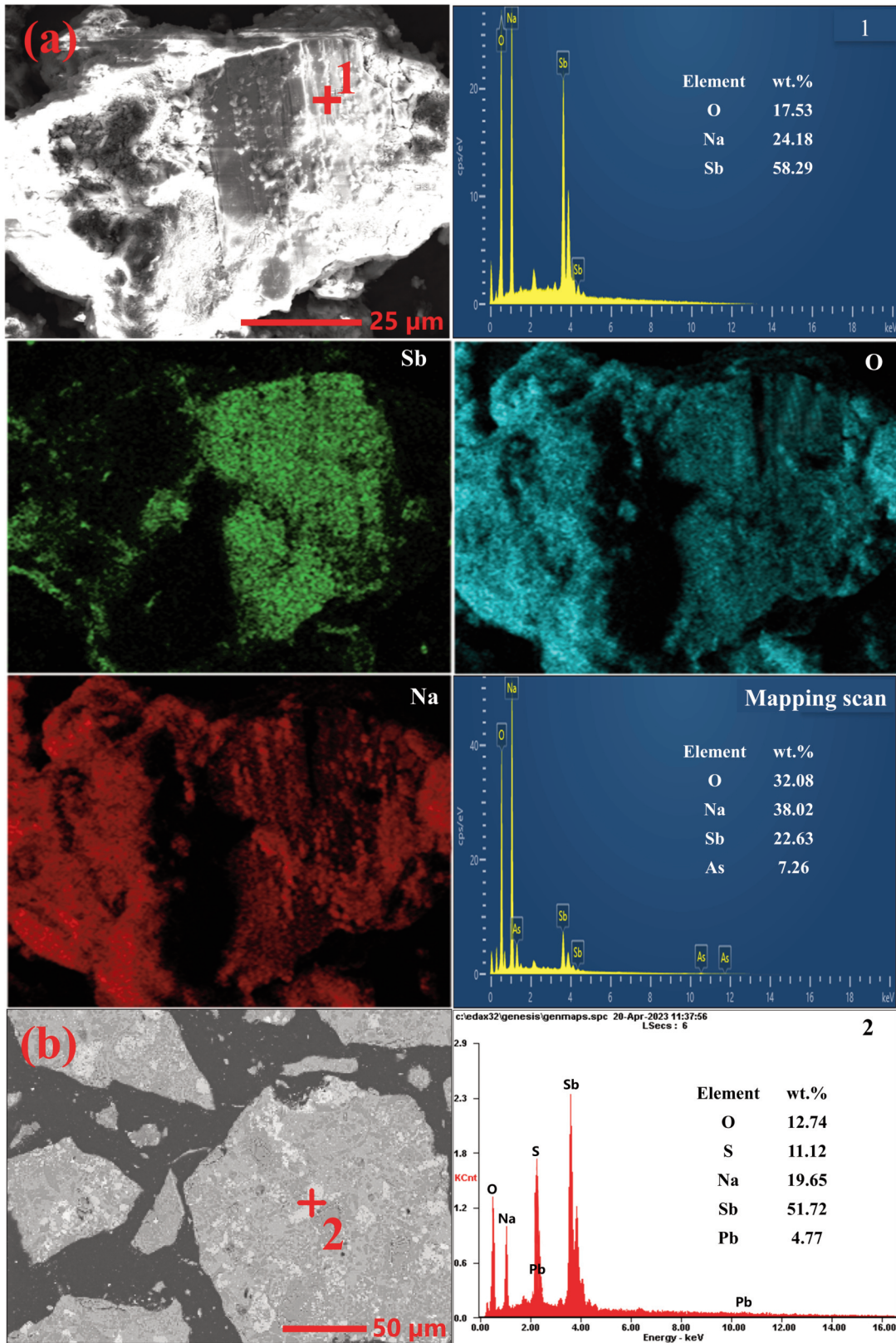
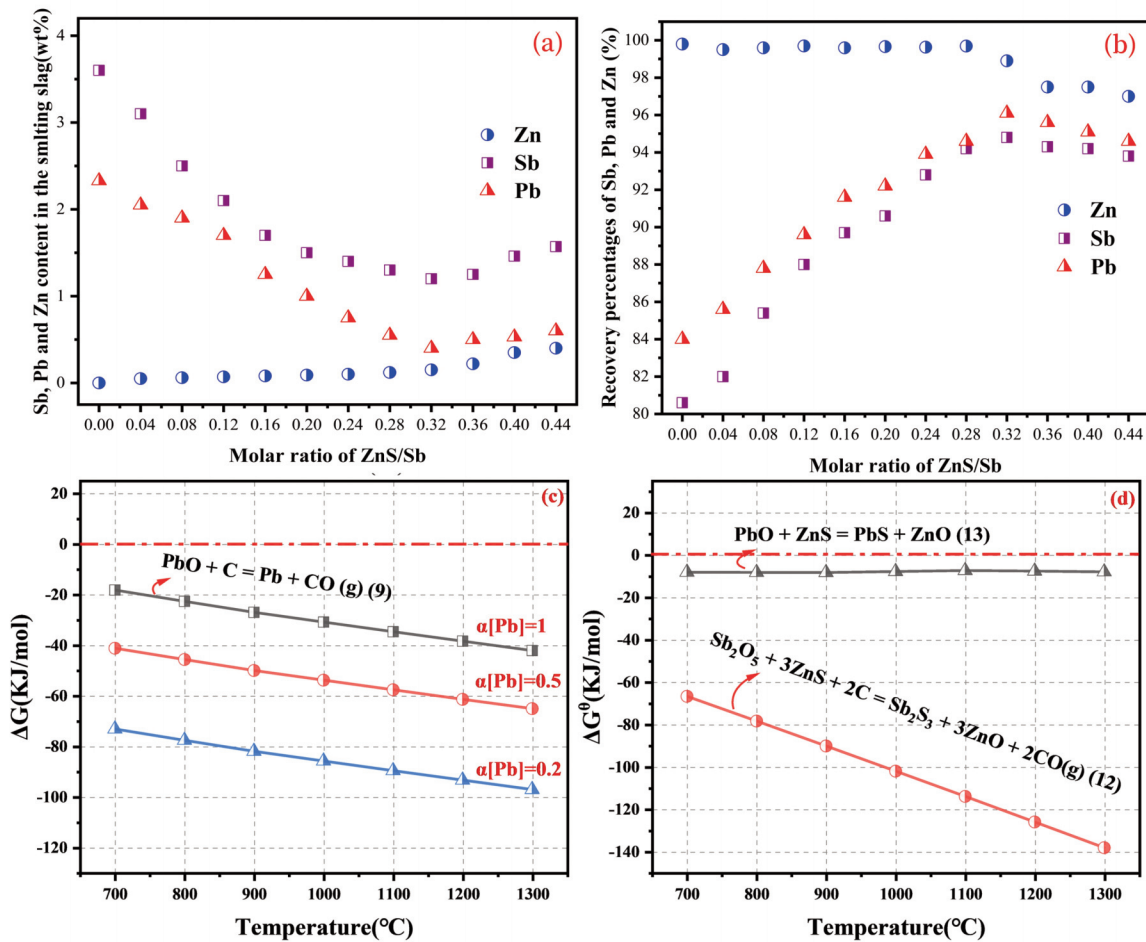


Figure 6. (a) SEM-EDS results of the smelting slag obtained in the absence of ZnS; (b) SEM-EDS results of the smelting slag obtained with a ZnS/Sb molar ratio of 0.40



**Figure 7.** (a) Effects of ZnS/Sb molar ratio on the Sb, Pb and Zn contents in the smelting slag; (b) Effects of ZnS/Sb molar ratio on the Sb, Pb and Zn recovery percentages from the As pre-removed lead anode slime; (c) Changes of Gibbs free energy ( $\Delta G$ ) of Eq. (9) at different Pb activities; (d) Changes of stand Gibbs free energy ( $\Delta G^0$ ) of Eqs. (12) and (13)

respectively, with the smelting temperature from 900 °C to 1200 °C (Fig. 8(a)). In addition, the increase of temperature also accelerated the volatilization of the generated Zn (g), causing that the Zn content in the smelting slag decreased in Figure 8(b). Though the Pb and Sb contents in the smelting slag changed little when the smelting temperature exceeded 1200 °C (Fig. 8(b)), the Pb and Sb yields decreased in Figure 8(a), which might be ascribed to the promotion on the volatilization of the generated Pb and the raw  $\text{Sb}_2\text{O}_3$  in the ARLAS at higher temperatures. The smelting temperature should be controlled at 1200 °C.

When the holding time increased from 30 min to 120 min, Figures 8(c) & (d) and Table 4 present that the yields of Pb, Sb and Zn increased to 96.1%, 94.8% and 98.9%, and the Pb, Sb and Zn contents in the smelting slag decreased to 0.38 wt%, 1.21 wt% and 0.14 wt% respectively. Then, all of them remained almost constant. The holding time was optimized to 120 min. In comparison with previous research [30],

the Sb yield from the ARLAS has an obvious increase in the presence of ZnS, from 86.89% to 94.8%. Tables 5 and 6 present the chemical composition of the obtained metal ingot and the distribution percentages of Sb, Pb and Zn in the metal ingot, smelting slag and dust respectively. It could be seen that Sb and Pb have been effectively recovered from the ARLAS and concentrated in a metal ingot. Meanwhile, the Zn from the added ZnS was recycled into a dust. Figures 8(e) and (f) show the XRD patterns of the obtained smelting slag and metal ingot respectively, which also indicated that Sb and Pb had been efficiently separated from the ARLAS and concentrated in a metal ingot. Little contents of valuable metals were contained in the smelting slag (Table 4), indicating it did not have recovery value. Moreover, there were soluble sodium salts (Fig.8(e)) in this slag, which were easy to be leached out and polluted environment. According to previous research, a vitrification technology could be used to achieve a harmless treatment [31].

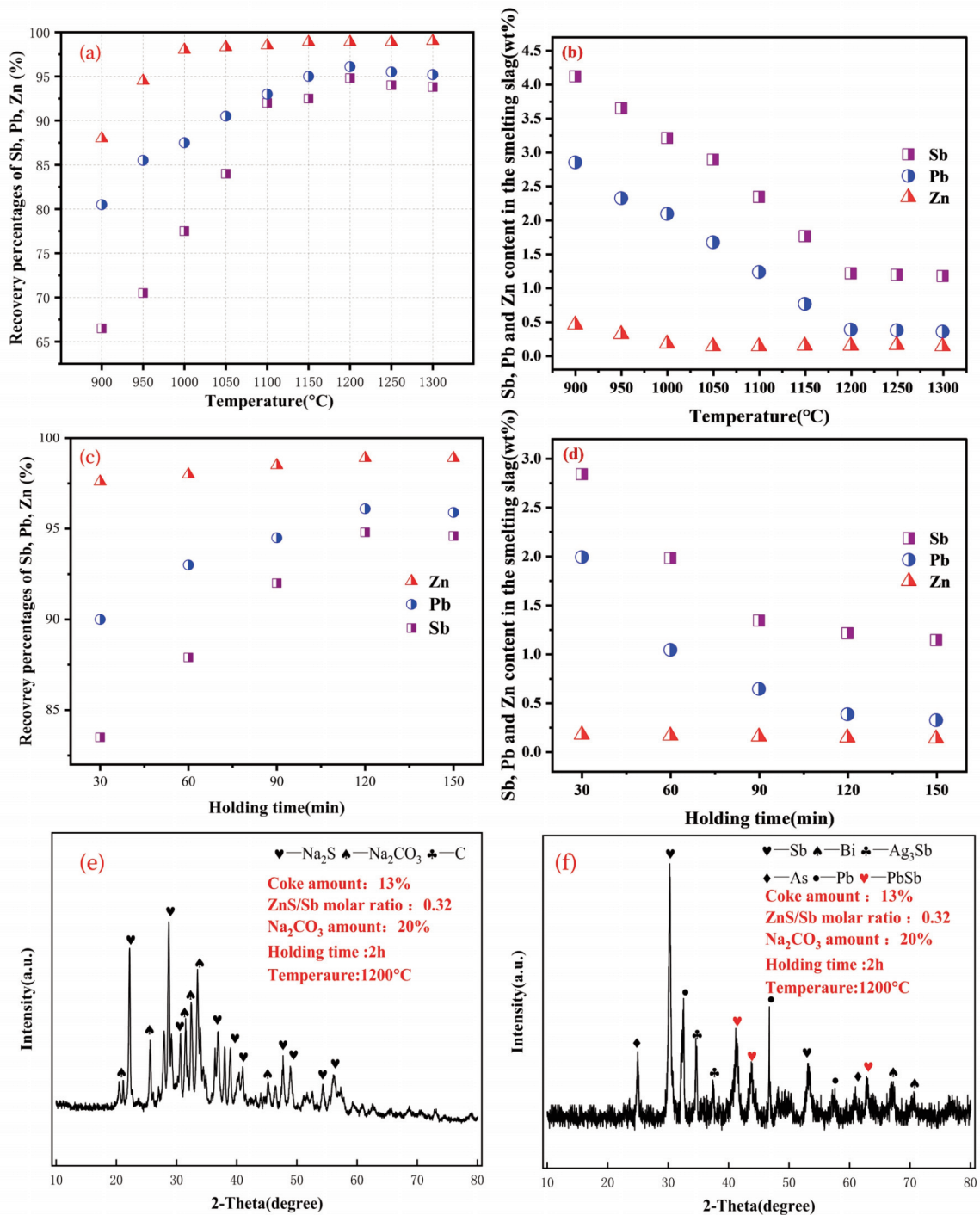


**Figure 8.** (a) Effects of smelting temperature on the Sb, Pb and Zn recovery percentages from the As pre-removed lead anode slime; (b) Effects of smelting temperature on the Sb, Pb and Zn contents in the smelting slag; (c) Effects of holding time on the Sb, Pb and Zn recovery percentages from the As pre-removed lead anode slime; (d) Effects of holding time on the Sb, Pb and Zn contents in the smelting slag; (e) XRD pattern of the smelting slag under the optimum condition; (f) XRD pattern of the metal ingot under the optimum condition

It is economically beneficial to increase the recovery percentages of Sb and Pb from the ARLAS using the ZnS- $\text{Na}_2\text{CO}_3$  smelting reduction proposed in this paper. The economic feasibility of this process

could be attributed to two aspects: 1) The addition of ZnS promoted the reduction of  $\text{Na}_3\text{SbO}_4$  and improved the recovery of Pb and Sb. Moreover, Zn in the ZnS could be recovered in a dust. 2) In

**Table 4.** Chemical composition of the smelting slag obtained at the optimized condition (wt%)

Element	Pb	As	Zn	Bi	S
Contents	0.38	2.12	0.14	0.21	16.62
Element	Sb	C	Na	O	Others
Contents	1.21	12.01	30.01	28.38	8.92

\*O content was detected by LECO TC-600 nitrogen/oxygen analyzer; S content was detected by elemental analyzer (EA, Vario Max CN); Other element contents were characterized by inductively coupled plasma optical emission spectroscopy (ICP-OES, Analytik Jena AG) and chemical analysis methods.

**Table 5.** Chemical composition of the metal ingot obtained at the optimized condition (wt%)

Element	Sb	Pb	Bi	As	Ag	Au	Others
Contents	52.93	24.34	6.78	7.45	6.62	0.05	1.83

\*Pb and Sb contents were characterized by chemical analysis, and the other element contents were detected by inductively coupled plasma optical emission spectroscopy (ICP-OES, Analytik Jena AG).

**Table 6.** The distribution percentages of Sb, Pb and Zn in the metal ingot, slag and dust at the optimum condition (%)

Element	Alloy	Slag	Dust
Sb	94.8	3.1	2.1
Pb	96.1	0.7	3.2
Zn	0.8	0.3	98.9

comparison with the general  $\text{Na}_2\text{CO}_3$  smelting reduction, the main additional cost was the ZnS consumption in the proposed process. While, the improvement of Pb and Sb recovery percentages has a higher value than this consumption, which could cover this cost.

## 5. Conclusion

In this study, an approach for the recovery of Sb from an As pre-removed lead anode slime using ZnS as additive was developed. The recycling of Pb from the slime and Zn from the added ZnS was also investigated.

After the As pre-removed lead anode slime was processed by ZnS- $\text{Na}_2\text{CO}_3$  smelting reduction, Sb, Pb and Zn were effectively recovered. ZnS promoted  $\text{Na}_3\text{SbO}_4$  reduction by destroying its stable structure and increasing its reductive activity. The recovered Sb and Pb were concentrated in a Pb-Sb alloy. Meanwhile, the added ZnS was reduced to volatile Zn (g), realizing Zn recycling after dust deposition. The results showed that the increasing the smelting temperature, holding time, coke and ZnS amount increased the recovery of Sb and Pb from the As pre-removed lead anode slime. Under the optimum conditions of a coke content of 13%, a ZnS/Sb molar ratio of 0.32, a smelting temperature of 1200 °C and holding time of 90 min, a yield of Sb, Pb and Zn of 94.8%, 96.1% and 98.9%, respectively, was achieved. However, an excess of ZnS reduced the yield of Pb and Sb, which was attributed to the formation of a sodium matte of Na-Pb-Sb-S.

## Author contributions

Zhunqin DONG: Data curation, Investigation, Validation, Writing – original draft. Rui ZHANG: Data curation, Investigation, Validation. Yixuan SUN: Investigation, Validation. Zhandong GU: Validation. Lei LI: Supervision, Writing – review & editing. Xueyi GUO: Supervision, Writing – review & editing. Songsong WANG: Writing – review & editing.

## Conflict of interest

The authors declare that they have no known competing financial interests or personal relationships that could have appeared to influence the work reported in this paper.

## Data availability

Data availability will be provided on request.

## Acknowledgments

The authors wish to express thanks to the National Natural Science Foundation of China (52174384) for the financial support of this research.

## References

- [1] W. Wang, S. Wang, J. Yang, C.S. Cao, K.W. Hou, L.X. Xia, J. Zhang, B.Q. Xu, B. Yang, Preparation of antimony sulfide and enrichment of gold by sulfuration–volatilization from electrodeposited antimony, *Minerals*, 12 (2) (2022) 264. <https://doi.org/10.3390/min12020264>
- [2] Z.T. Zhou, H.X. Xie, Y.Z. Wang, H. Xiong, S.P. Wang, L. Li, B.Q. Xu, B. Yang, High purity antimony sulfide condensate produced from heterogeneous antimony sulfide ore by directed volatilization in a vacuum ambient, *Minerals Engineering*, 191 (2023) 107983. <https://doi.org/10.1016/j.mineng.2022.107983>
- [3] I. Herath, M. Vithanage, J. Bundschuh, Antimony as a global dilemma: Geochemistry, mobility, fate and



- transport, *Environmental Pollution*, 223 (2017) 545-559. <https://doi.org/10.1016/j.envpol.2017.01.057>
- [4] L.A. Diaz, T.E. Lister, J.A. Parkman, G.G. Clark, Comprehensive process for the recovery of value and critical materials from electronic waste, *Journal of Cleaner Production*, 125 (2016) 236-244. <https://doi.org/10.1016/j.jclepro.2016.03.061>
- [5] L.G. Zhang, Z.M. Xu, A critical review of material flow, recycling technologies, challenges and future strategy for scattered metals from minerals to wastes, *Journal of Cleaner Production*, 202 (2018) 1001-1025. <https://doi.org/10.1016/j.jclepro.2018.08.073>
- [6] L. Li, M. Xu, Y. Xiao, Preparation of elemental As from As-Sb fly ash using continuous reductive method with additive of lead oxide, *Journal of Central South University*, 29 (2022) 3003-3015. <https://doi.org/10.1007/s11771-022-5146-y>
- [7] Y.M. Chen, N.N. Liu, L.G. Ye, S. Xiong, S.H. Yang, A cleaning process for the removal and stabilisation of arsenic from arsenic-rich lead anode slime, *Journal of Cleaner Production*, 176 (2018) 26-35. <https://doi.org/10.1016/j.jclepro.2017.12.121>
- [8] Z. Gao, X.F. Kong, B. Yang, J.F. Yi, K. Fan, T.Y. San, K.K. Cheng, S.X. Li, D.C. Liu, B.Q. Xu, W.L. Jiang, Extraction of scattered and precious metals from lead anode slime: A short review, *Hydrometallurgy*, 220 (2023) 106085. <https://doi.org/10.1016/j.hydromet.2023.106085>
- [9] J. F. Yi, K. K. Cheng, G. Z. Zha, K. Fan, S. X. Li, X. F. Kong, B. Yang, D. C. Liu, B. Q. Xu, An innovative green process for separating and enriching tellurium from lead anode slime via vacuum gasification, *Journal of Materials Research and Technology*, 16 (2022) 599-607. <https://doi.org/10.1016/j.jmrt.2021.12.060>
- [10] D.Q. Lin, K.Q. Qiu, Removal of Arsenic and Antimony from Anode Slime by Vacuum Dynamic Flash Reduction, *Environmental Science & Technology*, 45 (2011) 3361-3366. <https://doi.org/10.1021/es103424u>
- [11] X.X. Zhang, S. Friedrich, B. Friedrich, Separation behavior of arsenic and lead from antimony during vacuum distillation and zone refining, *Journal of Materials Research and Technology*, 9 (2020) 4386-4398. <https://doi.org/10.1016/j.jmrt.2020.02.063>
- [12] J.R. Xue, D.P. Long, H. Zhong, S. Wang, L.H. Liu, Comprehensive recovery of arsenic and antimony from arsenic-rich copper smelter dust, *Journal of Hazardous Materials*, 413 (2021) 125365. <https://doi.org/10.1016/j.jhazmat.2021.125365>
- [13] J.G. Yang, Y.T. Wu, A hydrometallurgical process for the separation and recovery of antimony, *Hydrometallurgy*, 143 (2014) 68-74. <https://doi.org/10.1016/j.hydromet.2014.01.002>
- [14] C.G. Anderson, Hydrometallurgically treating antimony-bearing industrial wastes, *JOM*, 53 (2001) 18-20. <https://doi.org/10.1007/s11837-001-0156-y>
- [15] P. Drahota, M. Filippi, Secondary arsenic minerals in the environment: A review, *Environment International*, 35 (2009) 1243-1255. <https://doi.org/10.1016/j.envint.2009.07.004>
- [16] A. Gong, X.G. Wu, J.H. Li, R.X. Wang, L.J. Chen, L. Tian, Z.F. Xu, Mechanism and kinetics for the carbothermal reduction of arsenic-alkali mixed salt produced from treatment of arsenic-alkali residue, *Thermochimica Acta*, 728 (2023) 179591. <https://doi.org/10.1016/j.tca.2023.179591>
- [17] H.B. Ling, M. Perin, B. Blanpain, M.X. Guo, A. Malfliet, Process flowsheet development for selective arsenic removal, lead and antimony recovery from lead softening slag, *Mineral Processing and Extractive Metallurgy Review*, (2023). <https://doi.org/10.1080/08827508.2022.2164575>
- [18] J.W. Han, Z.Y. Ou, W. Liu, F. Jiao, W.Q. Qin, Recovery of antimony and bismuth from tin anode slime after soda roasting-alkaline leaching, *Separation and Purification Technology*, 242 (2020) 116789. <https://doi.org/10.1016/j.seppur.2020.116789>
- [19] A. Gong, X.G. Wu, J.H. Li, R.X. Wang, J.C. Xu, S.H. Wen, Q. Yi, L. Tian, Z.F. Xu, Process and mechanism investigation on comprehensive utilization of arsenic-alkali residue, *Journal of Central South University*, 30 (2023) 721-734. <https://doi.org/10.1007/s11771-023-5253-4>
- [20] J.W. Han, W. Liu, W.Q. Qin, T.F. Zhang, Z.Y. Chang, K. Xue, Effects of sodium salts on the sulfidation of lead smelting slag, *Minerals Engineering*, 108 (2017) 1-11. <https://doi.org/10.1016/j.mineng.2017.01.007>
- [21] J.F. Yi, G.Z. Zha, D.X. Huang, X.F. Kong, B. Yang, D.C. Liu, B.Q. Xu, Effective separation and recovery of valuable metals from high value-added lead anode slime by sustainable vacuum distillation, *Journal of Cleaner Production*, 319 (2021) 128731. <https://doi.org/10.1016/j.jclepro.2021.128731>
- [22] L.M. Chen, Y.L. Zhen, G.H. Zhang, D.H. Chen, L.N. Wang, H.X. Zhao, F.C. Meng, T. Qi, Carbothermic reduction of vanadium titanomagnetite with the assistance of sodium carbonate, *International Journal of Minerals Metallurgy and Materials*, 29 (2022) 239. <https://doi.org/10.1007/s12613-020-2160-7>
- [23] W.D. Xing, S.H. Sohn, M.S. Lee, A Review on the Recovery of Noble Metals from Anode Slimes, *Mineral Processing and Extractive Metallurgy Review*, 41 (2021) 130-143. <https://doi.org/10.1080/08827508.2019.1575211>
- [24] K. Wang, Q.M. Wang, Y.L. En, Z.C. Li, X.Y. Guo, Antimony and arsenic substance flow analysis in antimony pyrometallurgical process, *Transactions of Nonferrous Metals Society of China*, 33 (2023) 2216-2230. [https://doi.org/10.1016/S1003-6326\(23\)66254-5](https://doi.org/10.1016/S1003-6326(23)66254-5)
- [25] Q. YI, A. Gong, J.C. Xu, S.H. Wen, Z.F. Xu, L. Tian, Preparation of arsenic-antimony from arsenic alkali residue by calcification transformation-carbothermal reduction, *Journal of Central South University*, 30 (2023) 2193-2204. <https://doi.org/10.1007/s11771-023-5379-4>
- [26] F.N. Han, L. Yu, G.H. Wen, Y.Y. Lu, L. Zhang, S.P. Gu, Comprehensive Understanding of the Role of Carbon Black in the Sintering and Melting Behavior of Mold Flux, *ISIJ International*, 62 (2022) 1657-1665. <https://doi.org/10.2355/isijinternational.ISIJINT-2022-078>
- [27] K.Z. Kourosh, R. Arifur, and J.B. Tang, Low Melting Temperature Liquid Metals and Their Impacts on Physical Chemistry, *Accounts of Materials Research*, 2 (2021) 577-580. <https://doi.org/10.1021/accountsmr.1c00143>
- [28] C.B. Tang, Y. Liu, L.G. Ye, Y.M. Chen, M.T. Tang, S.H. Yang, Production of bismuth by directly reducing-matting smelting from bismuth sulfide concentrate, *The Chinese Journal of Nonferrous Metals*, 27 (2017) 363-370. <https://doi.org/10.19476/j.ysxb.1004.0609.2017.02.017>



- [29] L. Li, M. Xu, Y. Xiao, Preparation of elemental As from As-Sb fly ash using continuous reductive method with additive of lead oxide, Journal of Central South University, 29 (2022) 3003-3015. <https://doi.org/10.1007/s11771-022-5146-y>.
- [30] H. Zhang, X.P. Ren, Process Design of Comprehensively Recycling Valuable Metals from Lead Anode Mud, Nonferrous Metals Design, 42 (2015) 17-20. (in Chinese)
- [31] Z.W. Zhao, Y.X. Song, X.B. Min, Y.J. Liang, L.Y. Chai, M.Q. Shi, XPS and FTIR studies of sodium arsenate vitrification by cullet, Journal of Non-Crystalline Solids, 452 (2016) 238-244. <http://dx.doi.org/10.1016/j.jnoncrysol.2016.08.028>

## DOBIJANJE Sb IZ OLOVNOG ANODNOG MULJA BEZ As REDUKCIJOM TOPLJENJA ZnS-Na<sub>2</sub>CO<sub>3</sub>

Z.-Q. Dong <sup>a,b</sup>, R. Zhang <sup>c</sup>, Y.-X. Sun <sup>c</sup>, Z.-D. Gu <sup>c</sup>, X.-Y. Guo <sup>a,\*</sup>, Lei Li <sup>c,\*\*</sup>, S.-S. Wang <sup>a</sup>

<sup>a</sup> Centralni južni univerzitet, Fakultet za metalurgiju i životnu sredinu, Čangša, Kina

<sup>b</sup> Shandong Humon Smelting CO., DOO, Jantaj, Kina

<sup>c</sup> Donghua Univerzitet, Fakultet za nauku o životnoj sredini i inženjering, Šangaj, Kina

### Apstrakt

Olovni anodni mulj se proizvodi u velikim količinama tokom elektrolize olova, ima visoki sadržaj Sb od 10-50 wt%, i on se može lako reciklirati. Međutim, u opštem procesu alkalnog luženja pod pritiskom za uklanjanje As, Sb se delimično konvertuje u Na<sub>3</sub>SbO<sub>4</sub> sa visokom stabilnošću. Ovo ograničava redukciju i izdvajanje Sb u narednoj Na<sub>2</sub>CO<sub>3</sub> redukciji topljenjem. Uzimajući u obzir ovu činjenicu, u ovoj studiji je kreativno korišćen ZnS kao aditiv za uništavanje stabilne strukture Na<sub>3</sub>SbO<sub>4</sub> i povećanje redukcije Sb, dok se ZnS redukuje u volatilni Zn (g) koji se reciklira. U određenom opsegu, povećanje količine koksa i ZnS povećava prinos Sb, a reciklaža Pb može biti ubrzana. Međutim, kada se doda prekomerna količina ZnS, Sb jedinjenja se mogu sulfurisati i zatim kombinovati sa generisanim PbS i Na<sub>2</sub>S, formirajući natrijumski mat Na-Pb-Sb-S. Ovo ograničava redukciju Sb i smanjuje prinos Sb. U optimalnim uslovima sa sadržajem koksa od 13%, molarnim odnosom ZnS/Sb od 0,32, temperaturom topljenja od 1200 °C i vremenom držanja od 90 minuta, postignuti su prinosi Sb, Pb i Zn do 94,8%, 96,1% i 98,9%, respektivno.

**Ključne reči:** Olovni anodni mulj bez prisustva As; Dobijanje Sb; ZnS; Transformacija faze; Redukcija topljenjem

